Journal of Ovarian Research

RESEARCH

Open Access

Gengnianchun formula ameliorates insulin resistance-induced diminished ovarian reserve via the estrogen signaling pathway: evidence from network pharmacology and experimental validation

Yanqiu Rao[1,2†], Jun Li[1,2†], Ting Xu[1,2], Lingyun Gao[1,2] and Wenjun Wang[1,2*]

Abstract

Background Diminished ovarian reserve (DOR), a major cause of female infertility, is closely linked to insulin resistance (IR). Traditional Chinese Medicine (TCM) approaches, such as the Gengnianchun (GNC) formula, focus on restoring ovarian function by improving IR and regulating hormonal balance. Despite GNC's demonstrated efficacy, its precise therapeutic mechanisms remain unclear.

Objective This study aims to elucidate the mechanisms by which GNC ameliorates IR-induced DOR through comprehensive pharmacological and experimental validation.

Methods The study combined Liquid chromatograph mass spectrometer (LC-MS), ultra-performance liquid chromatography (UPLC-TOF-MS/MS), network pharmacology, and molecular docking to identify active components and key therapeutic targets of GNC. Functional enrichment analyses (GO and KEGG) and molecular docking studies were performed. A high-fat diet-induced mouse model of IR-DOR was established, followed by GNC treatment at varying doses. Therapeutic effects were evaluated via qRT-PCR, western blot, immunofluorescence, and histological analysis.

Results GNC contains 219 active ingredients targeting 53 genes associated with IR-induced DOR. KEGG analysis revealed the estrogen signaling pathway as a key mechanism. High-dose GNC significantly improved IR and ovarian reserve by increasing AKT1, ESR1, and ESR2 expression, as confirmed by qRT-PCR, western blot and immunofluorescence analysis. These findings indicate that GNC enhances insulin sensitivity, promotes follicular development, and restores ovarian function.

†Yanqiu Rao and Jun Li contributed equally to this work.

*Correspondence:
Wenjun Wang
fduwjwwang@163.com

Full list of author information is available at the end of the article

Conclusions This study demonstrates for the first time that GNC alleviates IR-induced DOR by modulating the estrogen signaling pathway and activating key molecular targets. These results provide a foundation for clinical research and the development of novel therapeutic strategies for DOR.

Clinical trial number Not applicable

Keywords Gengnianchun formula, Insulin resistance, Diminished ovarian reserve, Network pharmacology, Estrogen signaling pathway

Background

Diminished ovarian reserve (DOR) refers to the decline in both the quantity and quality of oocytes and is a major cause of female infertility and poor response to controlled ovarian stimulation [1]. In recent years, the prevalence of DOR among patients undergoing assisted reproductive technology (ART) has risen from 19 to 26%, presenting an increasing challenge for reproductive medicine [2]. Beyond infertility, women with DOR also face a significantly higher risk of recurrent pregnancy loss [3]. The etiology of DOR is complex and multifactorial, with recent studies suggesting that the rising incidence of metabolic syndrome has severely impacted female reproductive health [4]. Insulin resistance (IR), the central pathological mechanism of metabolic syndrome, has also emerged as a key contributing factor to DOR [5].

IR is defined as a decreased responsiveness of tissues to insulin, resulting in compensatory hyperinsulinemia and impaired glucose metabolism [6]. Mechanistically, IR disrupts insulin signaling pathways within ovarian tissue, thereby compromising glucose metabolism and energy homeostasis, and inhibiting follicular growth and maturation [7]. Animal models subjected to high-fat diets have demonstrated that IR not only leads to hyperinsulinemia and dyslipidemia but also induces estrous cycle irregularities and reduces follicular reserve in mice [8]. DOR may be associated with mechanisms such as oxidative stress and inflammatory responses triggered by IR [9, 10]. Considering the close relationship between IR and DOR, there is an urgent need for effective therapeutic strategies that concurrently address both insulin sensitivity and ovarian function.

Current treatment for DOR primarily involves hormone replacement therapy (HRT), which aims to alleviate symptoms through the supplementation of exogenous estrogen. However, HRT does not significantly enhance ovarian reserve function and carries inherent risks [11]. In contrast, traditional Chinese medicine (TCM) provides a holistic therapeutic framework that emphasizes restoring of yin and yang balance, promoting qi circulation, and harmonizing the functions of the liver, spleen, and kidneys, thereby presenting a promising option for treating IR-induced DOR [12–14].

Gengnianchun (GNC) is a traditional Chinese herbal formula developed by three renowned traditional Chinese medicine practitioners from Shanghai, based on their extensive clinical experience and TCM theories. It comprises 12 herbal ingredients, including *Rehmannia glutinosa (Gaertn.) DC.* and *Epimedium acuminatum Franch.*, with treatment principles emphasizing kidney tonification, liver soothing, and heart clearing. GNC has been widely applied to enhance ovarian reserve and alleviate symptoms associated with DOR. In TCM, DOR induced by IR is characterized by kidney deficiency. GNC exhibits significant kidney-tonifying effects and has shown promising results in clinical practice, including enhancements in ovarian reserve, balancing reproductive endocrine status, and improving pregnancy and live birth rates [15]. Animal studies have also confirmed that GNC can significantly improve ovarian function in DOR mice induced by IR [16]. Although the efficacy of GNC has been established, the precise molecular mechanisms through which it exerts these effects remain incompletely understood.

To further elucidate the therapeutic mechanisms of GNC, this study employed Liquid chromatograph mass spectrometer (LC-MS) and ultra-performance liquid chromatography coupled with quadrupole time-of-flight mass spectrometry (UPLC-Q-TOF/MS) to identify the major bioactive components of GNC. Subsequently, network pharmacology was utilized to predict key molecular targets and pathways, which were further validated through molecular docking studies and experimental animal models. As illustrated in Fig. 1, this comprehensive approach provides a basis for understanding the molecular mechanisms by which GNC treats IR-induced DOR.

Materials and methods

Plant materials of GNC

The GNC herbs were obtained from Tianjiang Pharmaceutical Co. (Jiangyin, China), with specific details listed in Table 1. The plant names have been verified using the Medicinal Plant Names Services (MPNS) (http://mpns.kew.org). The extraction process followed the regulations and standards set forth in the Chinese Pharmacopoeia. From every 138 g of the original herbs, approximately 7.6 g of GNC granules were extracted.

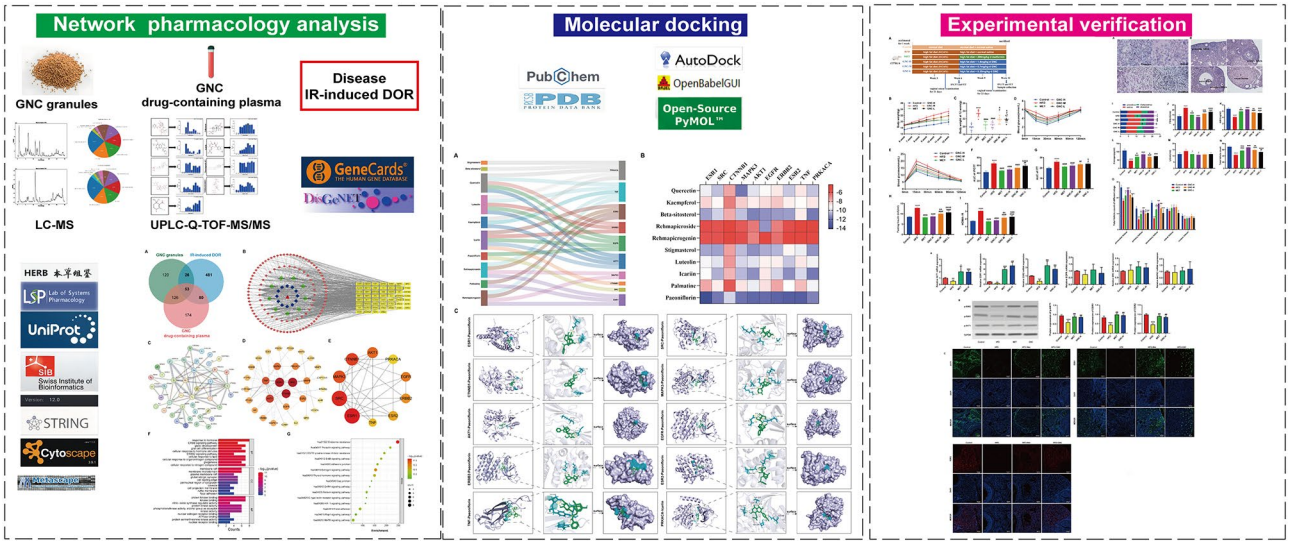

Fig. 1 Flowchart for the mechanism of action of GNC in the treatment of IR-induced DOR

Table 1 The details of GNC

Chinese Name	Accepted scientific name	Family	Plant Part	Crude Herb (g)
Shudihuang	Rehmannia glutinosa (Gaertn.) DC.	Orobanchaceae	Root	15
Yinyanghuo	Epimedium acuminatum Franch.	Berberidaceae	Root	12
Baishao	Paeonia lactiflora Pall.	Paeoniaceae	Root	12
Gouqizi	Lycium barbarum L.	Solanaceae	Fruit	12
Guiban	Plastrum Testudinis	Carapax	Carapax	15
Zhimu	Anemarrhena asphodeloides Bunge	Asparagaceae	Root	15
Tusizi	Cuscuta australis R.Br.	Convolvulaceae	Seed	12
Bajitian	Morinda officinalis F.C.How	Rubiaceae	Root	12
Congrong	Cistanche deserticola Y.C.Ma	Orobanchaceae	Stem	12
Huangbai	Phellodendron chinense C.K.Schneid.	Rutaceae	Bark	9
Huanglian	Coptis chinensis Franch.	Ranunculaceae	Rhizome	3
Fuling	Smilax glabra Roxb.	Smilacaceae	Sclerotium	9

LC-MS analysis

Mass spectrometry analysis was performed using a high-resolution 5600 QTOF mass spectrometer (AB SCIEX) coupled with an H-Class ultra-high performance liquid chromatography (UPLC) system (Waters). The sample preparation involved grinding the GNC, extracting with 75% methanol, and subsequent ultrasonic treatment. The analysis was conducted under both positive and negative ion modes, with the flow rate set at 400 µL/min and a gradient elution method. The electrospray ionization (ESI) source was operated at voltages of + 5500 V (positive) and – 4500 V (negative). The mass spectrometer collected data in the range of 50–1200 m/z, with an ionization energy of 30 eV for each cycle. The obtained data were processed using MSDIAL version 4.6, which involved peak detection, alignment, and identification by comparing the experimental results with databases such as Metlin, MassBank, and HMDB.

UPLC-Q-TOF-MS/MS analysis

To identify the active ingredients in GNC, plasma samples containing GNC were analyzed using UPLC-Q-TOF-MS/MS. Drug-containing plasma was prepared by orally administering GNC to female SD rats (230–260 g). The granules were dissolved in distilled water at a concentration of 0.5 g/mL, and each rat was dosed at 5 g/kg twice daily for three consecutive days. Blood samples were collected at multiple time points (0.25, 0.66, 1, 2, 4, 6, 8, and 10 h) after the final administration, with 0.2 mL of blood drawn at each interval. Plasma was separated by centrifuging the whole blood at 6,000 rpm for 8 min at room temperature and stored at – 80 °C until analysis.

Data were collected using a UPLC-MS/MS Vanskan Flash liquid chromatography system coupled with a Xevo G2-XS mass spectrometer (Waters Corp.,

Milford, MA, USA). Chromatographic analysis was performed on an ACQUITY UPLC BEH C18 column (2.1 × 100 mm, 1.7 μm) at 40 °C. The mobile phase consisted of water with 5 mM ammonium formate (A) and methanol (B), with a flow rate of 0.4 mL/min. The gradient elution program was as follows: 0–1 min (98% A, 2% B), 1–5 min (76% A, 24% B), 5–13 min (40% A, 60% B), 13–16 min (20% A, 80% B), 16–22 min (10% A, 90% B), and 22–25 min (98% A, 2% B). The injection volume was 10 μL. ESI was operated in both negative and positive ion modes, with molecular weight scanning set between 50 and 1000 Da. Collision-induced dissociation voltages were set at 6 V for low energy and 30–50 V for high energy.

Active compounds screening and prediction targets of GNC against IR-induced DOR

Active components of GNC were screened using the TCMSP (tcmspw.com/tcmsp.php) and the HERB database (herb.ac.cn/), based on ADME reference standards and Lipinski's rule. Compounds were selected if they met the criteria of oral bioavailability (OB) ≥ 30% and drug-likeness (DL) ≥ 0.18 [17]. Additionally, Lipinski's rule of five was applied to further refine the selection, including parameters such as molecular weight (Mw) ≤ 500 Da, LogP (miLogP) ≤ 5 (indicating appropriate lipophilicity), hydrogen bond donors (nOHNH) ≤ 5, and hydrogen bond acceptors (nOH) ≤ 10 [18]. The potential therapeutic targets of GNC drug-containing plasma were predicted using the SwissTargetPrediction database (www.swisstargetprediction.ch) and normalized using the UniProt database (www.uniprot.org/). IR and DOR-related genes were identified from GeneCards (www.genecards.org) and DisGeNET (www.disgenet.org/). Overlapping targets between the disease and drug were visualized using a Venn diagram [19].

Construction of herb-compound-intersection targets network

To identify key ingredients in GNC against IR-induced DOR, a herb-compound-intersection targets network was constructed using Cytoscape 3.9.1 software. The top 10 dominant compounds were determined based on their degree within the network.

Construction of protein–protein interaction (PPI) network

Overlapping gene targets were imported into the STRING database (string-db.org) to generate the protein-protein interaction (PPI) network. Cytoscape 3.9.1 software, along with the CytoHubba plugin, was utilized to identify the top 10 key genes from the PPI network.

GO and KEGG enrichment analysis

Gene Ontology (GO) and Kyoto Encyclopedia of Genes and Genomes (KEGG) enrichment analyses were conducted using Metascape (metascape.org). The top-ranked clusters, based on P-values, were visualized using bioinformatics tools (www.bioinformatics.com.cn).

Molecular Docking

Molecular docking was performed using AutoDock Tools, with the key active ingredients of GNC as ligands and core target proteins as receptors. The binding conformations were visualized using PyMOL software.

Animal model and treatment

Six-week-old female C57BL/6 mice were purchased from Shanghai Slack Laboratory Animal Co. Ltd. (License no: SCXK 2012-0002) and acclimatized in a Specific Pathogen Free(SPF) facility for 1 week. The mice had ad libitum access to food and water and were maintained under a 12-hour light/dark cycle. Mice were divided into a control group (Control, $n = 8$) on a normal diet, and an experimental group on a high-fat diet (HFD, Cat. No.: D12451, Research Diets) for 6 weeks to induce IR and DOR. After 3 weeks, vaginal smears were performed daily for 21 days to monitor estrous cycles.

At 6 weeks, intraperitoneal glucose tolerance tests(IPGTT) and insulin tolerance tests (ITT) were performed to confirm the establishment of the IR-induced DOR model. Mice in the experimental group were then randomized into five groups: HFD group, Metformin group (200 mg/kg), and GNC groups with high (1.4 mg/kg), medium (0.7 mg/kg), and low doses (0.35 mg/kg) ($n = 8$ per group). Dosages were based on a previous study (Peng et al., 2023). GNC and metformin were administered via oral gavage for 6 weeks, with dosages adjusted according to weekly body weight. Control and HFD groups received equivalent volumes of solvent. After 6 weeks of treatment, vaginal smears, IPGTT, and ITT were repeated. Mice were sacrificed after the non-estrus phase or when fasting was completed, and serum and ovarian tissue were collected for analysis. All animal experiments were approved by Institutional Animal Care and Use Committee of SHZY (permit No.: SHZY-202307FT).

Estrous cycle examination

Vaginal smears were collected daily at the same time to monitor the estrous cycle of the mice. A pipette containing 10 μL of saline was used to collect vaginal samples, which were then stained with Wright-Giemsa and examined under a light microscope. The estrous cycle was categorized into four phases based on the predominant cell types observed in the vaginal smears: proestrus, estrus, metestrus, and diestrus.

IPGTT and ITT test

The intraperitoneal glucose tolerance test (IPGTT) was conducted by administering an intraperitoneal injection of glucose at a dose of 2 g/kg body weight following a 16-hour fast. The insulin tolerance test (ITT) involved injecting insulin intraperitoneally at a dose of 0.75 U/kg body weight after a 4-hour fast in mice. Glucose concentrations were measured through tail vein blood sampling at 0, 15, 30, 60, 90, and 120 min.

Serum hormone and insulin assay

LH (CUSABIO, CSB-E12770m), FSH (CUSABIO, CSB-E06871m), E2 (CUSABIO, CSB-E07280m), AMH (CUSABIO, CSB-E13156m), and insulin (Mlbio, ml001983) levels were measured using ELISA kits according to the manufacturer's instructions. Each group consisted of eight samples, and each experiment was replicated three times. The inter- and intra-batch variability for each kit was less than 15%. HOMA-IR was calculated using the formula: HOMA-IR = fasting blood glucose(FBG) × fasting serum insulin(FINS) / 22.5.

Histological analysis and follicle counts

Ovarian tissues were fixed in 4% paraformaldehyde, embedded in paraffin, and then serially sectioned at 4 μm thickness. The sections were stained with hematoxylin and eosin (H&E) for follicle counting. The average number of follicles was recorded from five different sections of each ovary under a microscope. Follicles were categorized into four developmental stages according to the modified Oktay system [20]. The counting process was repeated three times by different researchers to ensure accuracy.

Quantitative real-time PCR (qRT-PCR)

Total RNA was extracted from ovarian tissue using the RNA Purification Kit PLUS (RN001-plus, EZBioscience) and subsequently converted into complementary DNA (cDNA) using the Color Reverse Transcription Kit (A0010CGQ, EZBioscience). The primer sequences used for qRT-PCR are listed in Supplementary Table S1. Gene expression levels were quantified using the comparative cycle threshold (Ct) method (2^(-ΔΔCt)), with target gene Ct values normalized to those of the housekeeping gene.

Western blotting

Ovarian tissues from the Control, HFD, MET, and GNC treatment groups were homogenized in RIPA buffer containing protease and phosphatase inhibitors. Protein concentrations were measured using the BCA protein assay kit (Thermo Fisher Scientific, USA). Equal amounts of protein (30 μg) from each sample were separated by 10% SDS-PAGE and transferred onto a PVDF membrane (Millipore, Burlington, USA). The membrane was blocked with 5% non-fat milk in TBS-T for 1 h at room temperature, followed by overnight incubation with primary antibodies at 4 °C. The primary antibodies used included: anti-phospho-AKT (1:1,000, Proteintech), anti-phospho-ESR1 (1:1,000, Proteintech), and anti-phospho-ESR2 (1:1,000, Proteintech). The membranes were then incubated with HRP-conjugated secondary antibodies (1:5,000, Santa Cruz Biotechnology) for 1 h at room temperature. Protein bands were visualized using chemiluminescence detection, and expression levels were quantified with ImageJ software, with GAPDH (1:5,000, Proteintech) as the internal control.

Immunofluorescence

Ovarian tissue sections were deparaffinized, rehydrated, and subjected to antigen retrieval. The sections were blocked with PBS containing 3% bovine serum albumin (BSA) for 30 min at room temperature, then incubated with primary antibodies against AKT1 (Proteintech Group, Inc.), ESR1 (Proteintech Group, Inc.), and ESR2 (Thermo Scientific, Waltham, MA, USA), each at a 1:100 dilution. After washing in PBS, the sections were incubated with secondary antibodies for 1 h at room temperature, followed by incubation in DAPI staining solution (G1012, Servicebio) for 10 min. Immunofluorescence was detected and images were captured using a fluorescence microscope.

Statistical analysis

All data are presented as mean ± standard deviation (SD). Statistical analyses were conducted using GraphPad Prism version 10.1. For comparisons between two groups, an independent unpaired t-test was performed for normally distributed data with equal variances, and the Mann-Whitney U test was applied for non-normally distributed data. For multiple group comparisons, ANOVA followed by Dunnett's post-hoc test was used to assess differences among groups with equal variances. In cases where the assumption of homogeneity of variances was violated, Welch's ANOVA was conducted, followed by the Games-Howell post-hoc test for pairwise comparisons. Categorical and proportion data, such as the distribution of estrous cycle phases, were analyzed using the chi-square test for multiple independent groups. A p-value of less than 0.05 was considered statistically significant for all analyses.

Results

Mass spectrometry detection of GNC

Metabolomic analysis of GNC was conducted using LC-MS in both positive and negative ionization modes to comprehensively profile its chemical composition. The Total Ion Current (TIC) chromatograms, shown

in Fig. 2A (positive ion mode) and Fig. 2B (negative ion mode), reveal the chemical complexity of GNC, with distinct peaks observed across a 0–30 min retention time range. In positive ion mode, the TIC chromatogram exhibited high-intensity signals, with prominent peaks observed between 5 and 20 min. These peaks correspond to lipophilic compounds, such as flavonoids and alkaloids, which are positively ionizable and are typically associated with antioxidant and anti-inflammatory activities. In negative ion mode, the TIC chromatogram displayed distinct peaks with moderate intensity, primarily corresponding to organic oxygen compounds and lignans, which are typically negatively charged. This mode revealed additional metabolic components, complementing the findings from the positive ion mode and providing a more holistic view of the chemical diversity present in GNC. The identification of phenolic acids and glycosides, compounds known for their anti-inflammatory and hormonal regulation effects, further substantiates GNC's therapeutic potential in addressing insulin resistance and promoting ovarian health.

Chemical composition analysis of GNC drug-containing plasma

UPLC-Q-TOF/MS was utilized to identify the active chemical components in the plasma of rats treated with GNC. Nine components were detected and absorbed into rat plasma following GNC gavage, including paeoniflorin, palbinone, berberine, icariin, timosaponin E2, timosaponin A1, rehmannioside C, rehmannioside D, and rehmapicroside. The structural information and chemical profiles of these nine compounds are presented in Fig. 2C; Table 2, respectively. These compounds exhibited specific peaks that corresponded to their respective absorption profiles, with varying intensities observed at different time points post-administration. These results indicate their bioavailability and absorption dynamics following oral administration.

Network Pharmacology of GNC treating IR-induced DOR

Construction of drug-compound-intersection targets-disease network

Based on the molecular structures derived from UPLC-Q-TOF/MS analysis, a total of 325 potential targets were predicted using the SwissTargetPrediction database. A total of 210 active compounds of GNC granules were identified through screening from the TCMSP and HERB databases, with 433 target genes retrieved from the UniProt database. Additionally, 4280 genes related to IR and 709 genes related to DOR were identified from GeneCards and DisGeNet databases, respectively. A Venn diagram analysis identified 53 overlapping targets associated with GNC, IR, and DOR (Fig. 3A), with detailed information provided in Supplementary Table S2.

These 53 overlapping genes were subsequently imported into Cytoscape 3.9.1 to construct a drug-compound-intersecting targets-disease network, consisting of 182 nodes and 84 edges (Fig. 3B). The top 10 active compounds of GNC, ranked by their degree values, were quercetin, kaempferol, beta-sitosterol, rehmapicroside, rehmapicrogenin, stigmasterol, luteolin, epimedium, palmatine, and paeoniflorin, indicating their critical roles in GNC's therapeutic effects on IR-induced DOR (Table S3).

Construction of protein–protein interaction (PPI) network

A PPI network of the 53 overlapping genes was constructed using the STRING database, consisting of 53 nodes and 71 edges, with an average of 2.68 edges per node (Fig. 3C). The PPI network was subsequently analyzed using Cytoscape 3.9.1, and node color and size were adjusted based on the degree value, nodes with higher degree values were assigned darker colors, while edge thicknesses were proportional to these values (Fig. 3D). The CytoHubba plugin in Cytoscape identified the top 10 core genes based on the maximum clique centrality(MCC) method (Fig. 3E), with ESR1, SRC, CTNNB1, MAPK3, AKT1, EGFR, ERBB2, ESR2, TNF, and PRKACA recognized as the most critical targets (Table S4).

GO and KEGG pathway analysis of overlapping genes

GO and KEGG enrichment analyses were performed using Metascape. The top 10 terms in biological processes (BP), cellular components (CC), and molecular functions (MF) categories from the GO analysis are presented in Supplementary Table S5. The GO analysis revealed that biological processes associated with GNC predominantly involve hormonal responses, while its effects on cellular components are focused on membrane rafts, and its molecular functions are linked to nuclear receptor activity (Fig. 3F). The KEGG pathway enrichment analysis, illustrated as a bubble diagram in Fig. 3G, identified key pathways, including endocrine resistance, estrogen signaling, and thyroid hormone signaling as potential intervention pathways for GNC in IR-induced DOR (Table S6).

Molecular Docking of key components and targets

The sankey plot analysis of 10 core bioactive components and 10 core target genes of GNC indicated that all were interconnected. Consequently, molecular docking experiments were performed to verify the results. Docking results demonstrated strong binding interactions, with all ligands exhibiting binding energies below 5 KJ/mol, indicative of stable interactions (Fig. 4A). Among the docked compounds, paeoniflorin and icariin demonstrated the most stable interactions with key genes, with paeoniflorin showing the lowest binding energies with

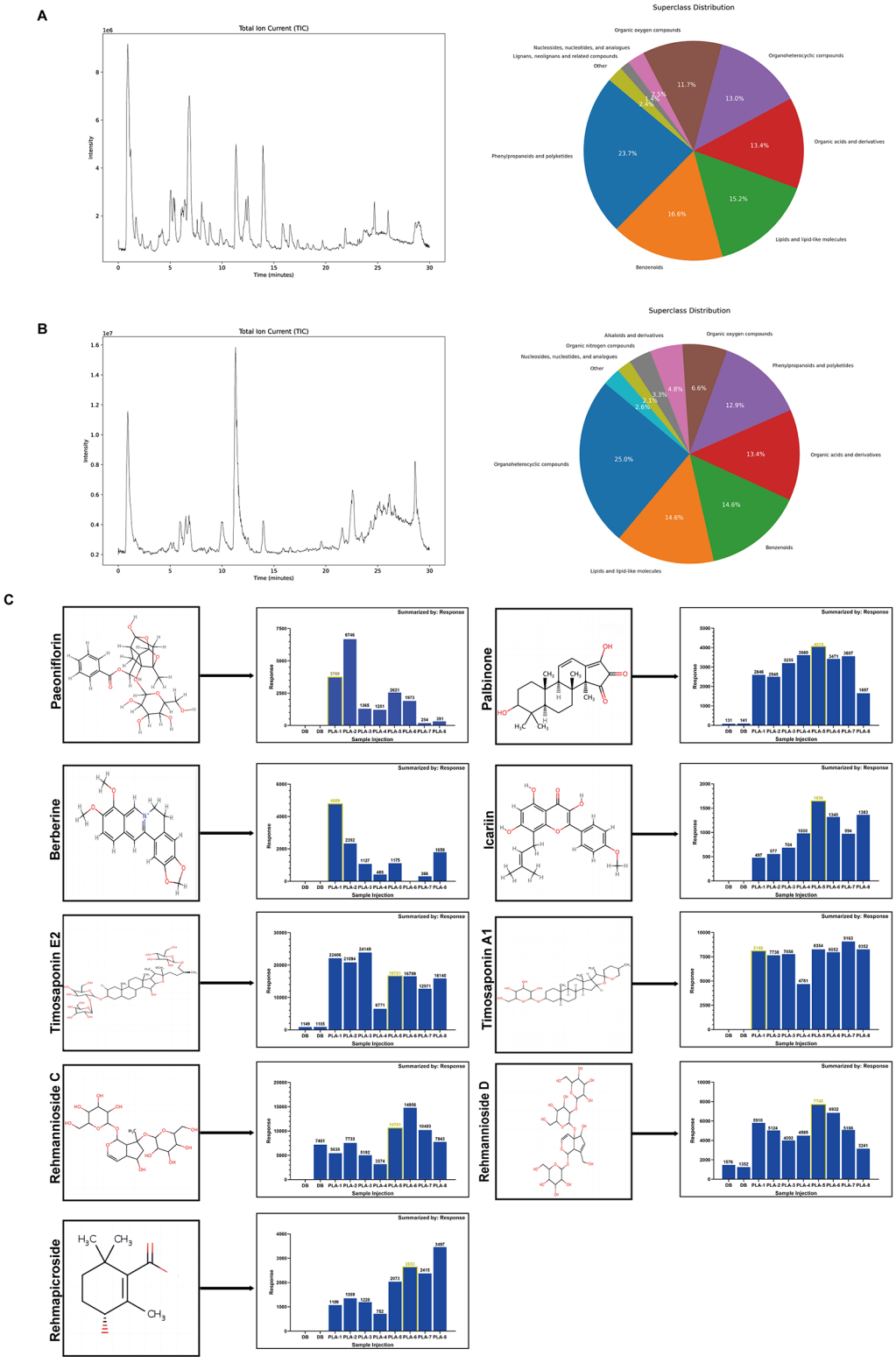

Fig. 2 Chemical composition analysis of GNC by LC-MS and UPLC-Q-TOF-MS/MS. (**A**) Total Ion Current (TIC) chromatogram of GNC in positive ion mode, displaying distinct high-intensity peaks, primarily between 5 and 20 minutes, corresponding to lipophilic compounds such as flavonoids and alkaloids. (**B**) TIC chromatogram of GNC in negative ion mode, showing moderate intensity peaks corresponding to organic oxygen compounds and lignans. (**C**) UPLC-Q-TOF-MS/MS analysis of drug-containing plasma from rats administered GNC, identifying nine active compounds. These peaks correspond to specific compounds, indicating their absorption and bioavailability in plasma at various time points post-administration

Table 2 UPLC-Q-TOF-MS/MS analysis of GNC drug-containing plasma in rats

	Molecule Name	Source	Molecluar Formula	tR/min	Ion	M/Z
1	Paeoniflorin	Radix Paeoniae Alba	$C_{23}H_{28}O_{11}$	6.35	M + Na	503.1526
2	Palbinone	Radix Paeoniae Alba	$C_{22}H_{30}O_4$	16.26	M-H	357.2038
3	Berberine	Rhizoma Coptidis	$C_{20}H_{18}NO_4$	8.46	M + H	336.123
4	Icariin	Epimedium Brevicornums	$C_{21}H_{20}O_6$	11.67	M-H	367.118
5	Timosaponin E2	Rhizoma Anemarrhenae	$C_{46}H_{79}O_{20}$	16.08	M + H	951.5183
6	Timosaponin A1	Rhizoma Anemarrhenae	$C_{33}H_{54}O_8$	18.6	M + Na	601.3715
7	Rehmannioside C	Rehmanniae Radix Praeparate	$C_{21}H_{35}O_{14}$	19.47	M + H	511.2029
8	Rehmannioside D	Rehmanniae Radix Praeparate	$C_{27}H_{42}O_{20}$	17.05	M + Na	709.2145
9	Rehmapicroside	Rehmanniae Radix Praeparate	$C_{10}H_{16}O_3$	11.48	M + Na	207.0991

CTNNB1, AKT1, EGFR, ERBB2, SRC, ESR2, MAPK3, ESR1, and TNF, and icariin binding most stably with PRKACA (Fig. 4B, C). The binding energy results are shown in the Supplementary Table S8.

Experimental validation based on network Pharmacology

GNC ameliorates insulin resistance in IR-induced DOR mice

The experimental design is illustrated in Fig. 5A. At the beginning of the study, no significant differences in body weight were observed between groups. However, after six weeks of a high-fat diet, both body weight and the area under the curve(AUC) values from the IPGTT and ITT tests in the HFD group were significantly elevated compared to the Control group, indicating the successful establishment of the IR-induced DOR model (Supplementary Fig. 1, $p < 0.01$). Following treatment with GNC or metformin, body weight gain was significantly reduced across all treatment groups, with some groups even showing weight loss (Fig. 6B, $p < 0.05$). At the end of the experiment, body weight, IPGTT/ITT AUC, FINS, and HOMA-IR values were all significantly lower in the GNC and MET groups compared to the HFD group (Fig. 6B-I, $p < 0.05$). The dose-dependent effect of GNC was evident, with GNC-H showing the most significant improvement in insulin sensitivity.

GNC improves ovarian function in IR-induced DOR mice

Changes in vaginal smears at different stages of the estrous cycle and follicular morphology are illustrated in Fig. 5A-H. After six weeks of a high-fat diet, the estrous period was significantly shortened, and the diestrus period was extended in the HFD group compared to the Control group, indicating reduced ovarian function (Supplementary Fig. 1F, $p < 0.01$). Treatment with GNC and metformin restored the estrous cycle, lengthening the estrous phase and shortening the diestrus phase compared to the HFD group (Fig. 5I, $P < 0.01$). Additionally, FSH levels were elevated, whlie E_2 and AMH levels decreased in the HFD group; these changes were reversed following treatment with GNC or metformin (Fig. 5J-L, $P < 0.01$). GNC-H and GNC-M groups also showed significantly lower LH levels (Fig. 5M, $P < 0.05$). Furthermore, counts of primordial, primary, and secondary follicle were significantly higher in the GNC and MET groups compared to the HFD group (Fig. 5O, $P < 0.05$), and total follicle counts were also elevated (Fig. 5N, $P < 0.01$). Notably, the GNC-H was superior to other doses in improving FSH, E_2, AMH, and follicle counts, suggesting a dose-dependent effect of GNC on the improvement of ovarian function.

GNC activates the Estrogen signaling pathway

Given that the GO enrichment analysis identified hormone response as the most significantly affected biological process, and the KEGG analysis highlighted estrogen signaling as a key pathway, we further investigated the expression of genes with this pathway. qRT-PCR analysis demonstrated that the mRNA levels of AKT1, ESR1 and ESR2 were significantly downregulated in the HFD group, but were markedly restored following GNC and MET treatments (Fig. 7A, $P < 0.05$). To substantiate these findings at the protein level, Western blot (WB) analysis was performed on ovarian tissue samples from the same experimental groups. As shown in Fig. 7B, the protein expression levels of p-AKT1, p-ESR1, and p-ESR2 were significantly upregulated in both the GNC and MET treatment groups compared to the HFD group. These results indicate that GNC activates the estrogen signaling pathway at the protein level. Additionally, immunofluorescence (IF) staining of ovarian tissue further corroborated these findings, demonstrating enhanced expression of AKT1, ESR1, and ESR2 in the GNC and MET treatment groups (Fig. 7C). These findings provide compelling evidence that GNC exerts its protective effects through the activation of the estrogen signaling pathway, supporting its potential as a therapeutic strategy for improving ovarian reserve and function.

Discussion

DOR significantly impacts women's reproductive health and quality of life, highlighting the critical need for early and effective intervention. IR, often exacerbated by

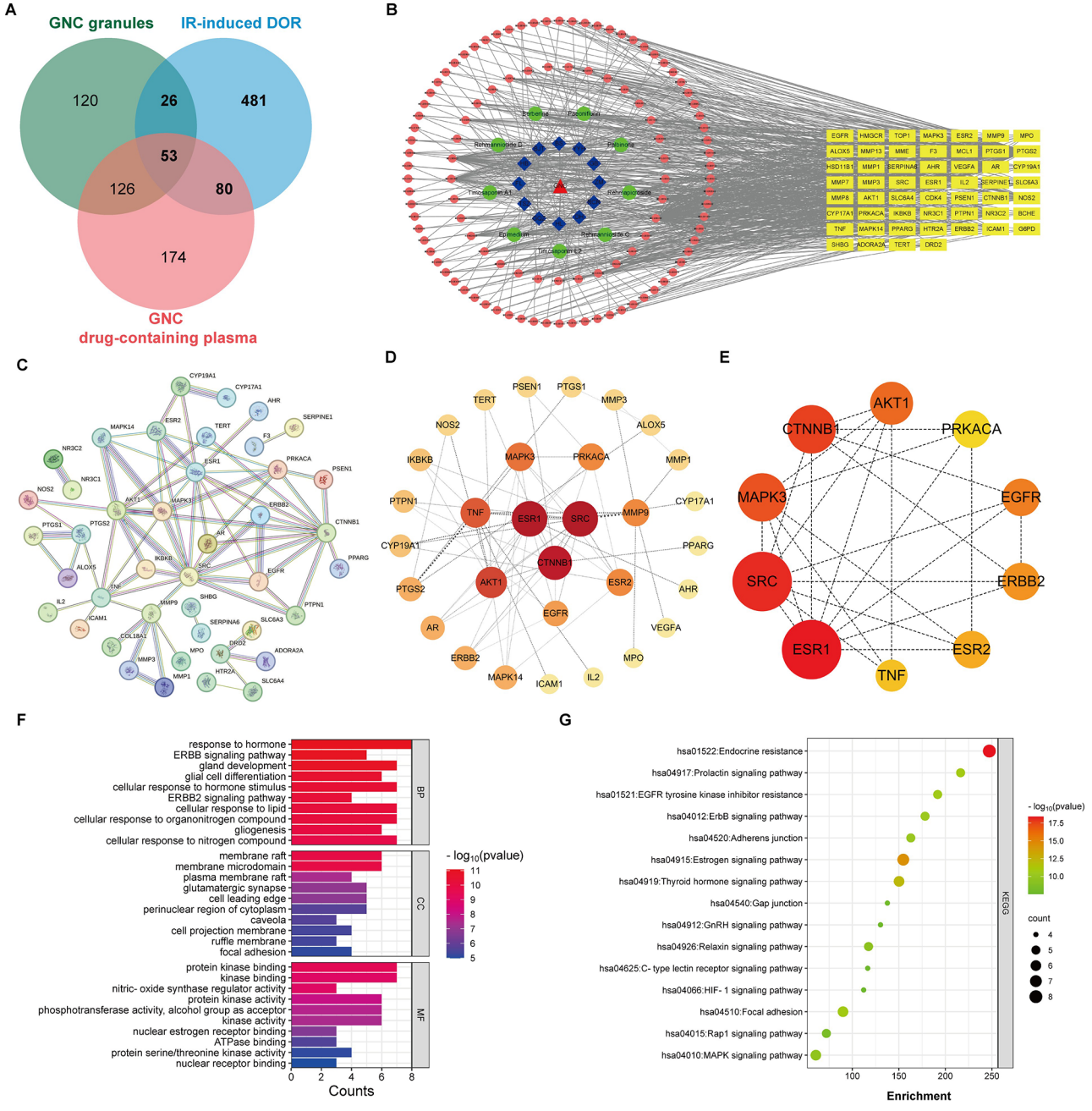

Fig. 3 Network Pharmacology Analysis of GNC in Treating IR-Induced DOR. (**A**) Venn diagram illustrating 53 overlapping target genes among GNC granules, GNC drug-containing plasma, and IR-induced DOR-related genes, representing potential therapeutic targets. (**B**) GNC-compound-intersecting targets-disease network illustrating the connections between compounds and disease targets. Blue squares represent individual herbs in the GNC formula, green circles indicate bioactive compounds detected in plasma, pink circles denote bioactive ingredients, and yellow squares correspond to the intersection genes linked to both GNC and IR-induced DOR. (**C**) PPI network of 53 potential targets from the STRING database. (**D**) PPI network visualization with node size and color depth indicating target degree. (**E**) Identification of top 10 core genes in the PPI network using the CytoHubba plugin. The node color ranged from pale yellow to red, with the corresponding degree gradually increasing.(**F**) GO Enrichment Analysis of biological processes, cellular components, and molecular functions, with the x-axis representing gene ratio and color gradient indicating statistical significance. (**G**) KEGG Pathway Enrichment Analysis showing key pathways like the estrogen signaling pathway; the x-axis indicates enrichment scores, bubble size reflects gene counts, and color gradient denotes p-value significance

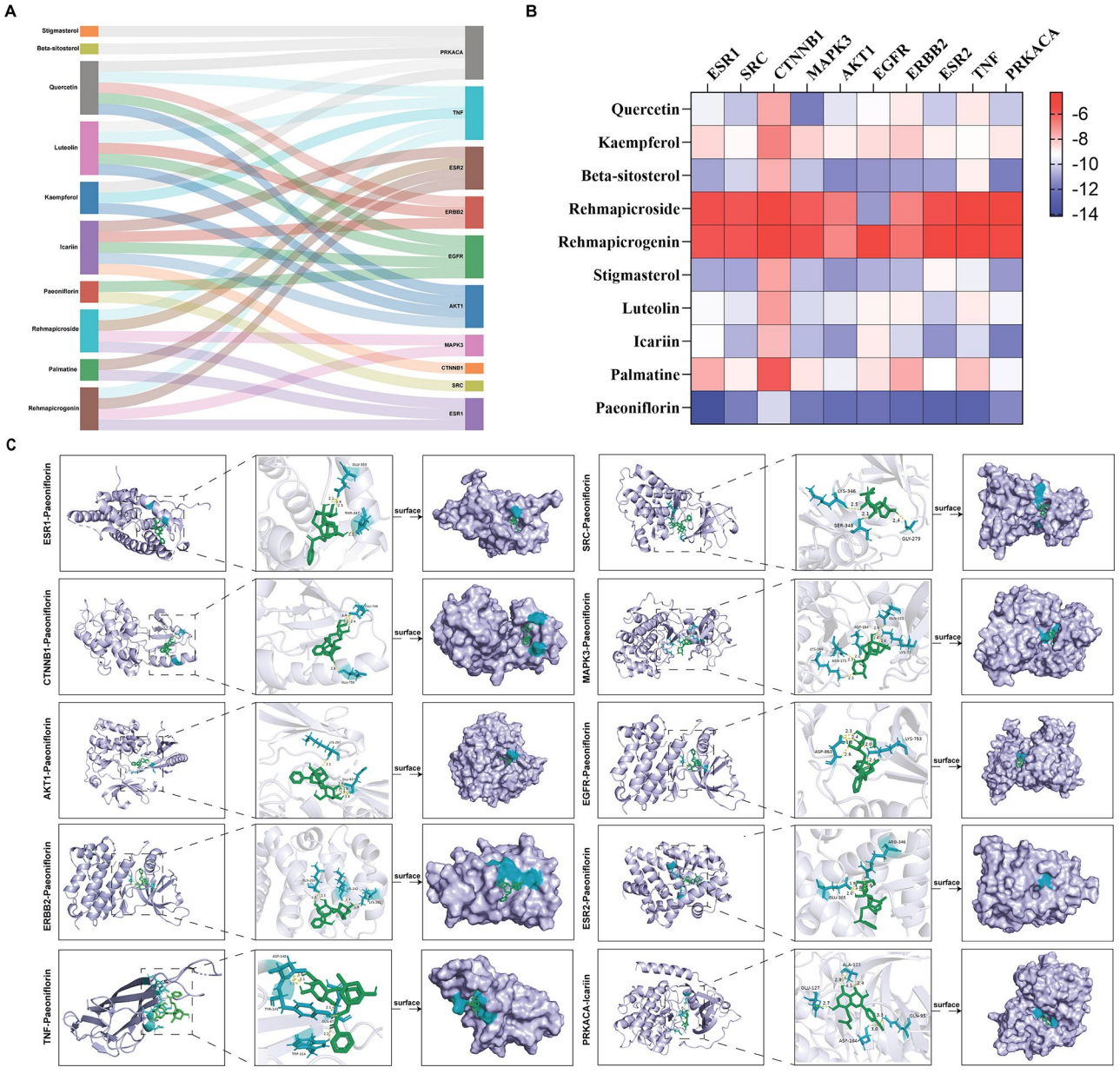

Fig. 4 Molecular docking of bioactive components with key target proteins. (**A**) Sankey plot illustrating the relationship between bioactive components and their target proteins. (**B**) Heat map of the docking interactions, highlighting binding energies. (**C**) Docking modes of the bioactive components with the target proteins, demonstrating stable binding interactions

high-calorie diets, is a key contributor to the rising incidence of metabolic dysfunction, which adversely affects female reproductive health [21, 22]. While traditionally associated with polycystic ovary syndrome (PCOS), recent studies also suggest that IR directly impairs ovarian reserve [23]. Preliminary experiments conducted by our research group have confirmed that GNC can enhance insulin sensitivity and ovarian function in a mouse model of IR-induced DOR. Nevertheless, the molecular mechanisms through which GNC exerts these effects remain incompletely understood [16]. This study aimed to elucidate these mechanisms by utilizing LC-MS and UPLC-Q-TOF-MS/MS analyses to identify key bioactive compounds, alongside network pharmacology to predict potential molecular targets. These integrative approaches offer a comprehensive understanding of how GNC ameliorates IR-induced DOR at the molecular level.

The LC-MS and UPLC-Q-TOF-MS/MS analyses provided a detailed characterization of the bioactive compounds in GNC and their pharmacokinetic behavior. Mass spectrometry analysis of the GNC revealed several bioactive compounds, many of which are known to improve IR and DOR. In positive ion mode, lipophilic compounds such as flavonoids and alkaloids were

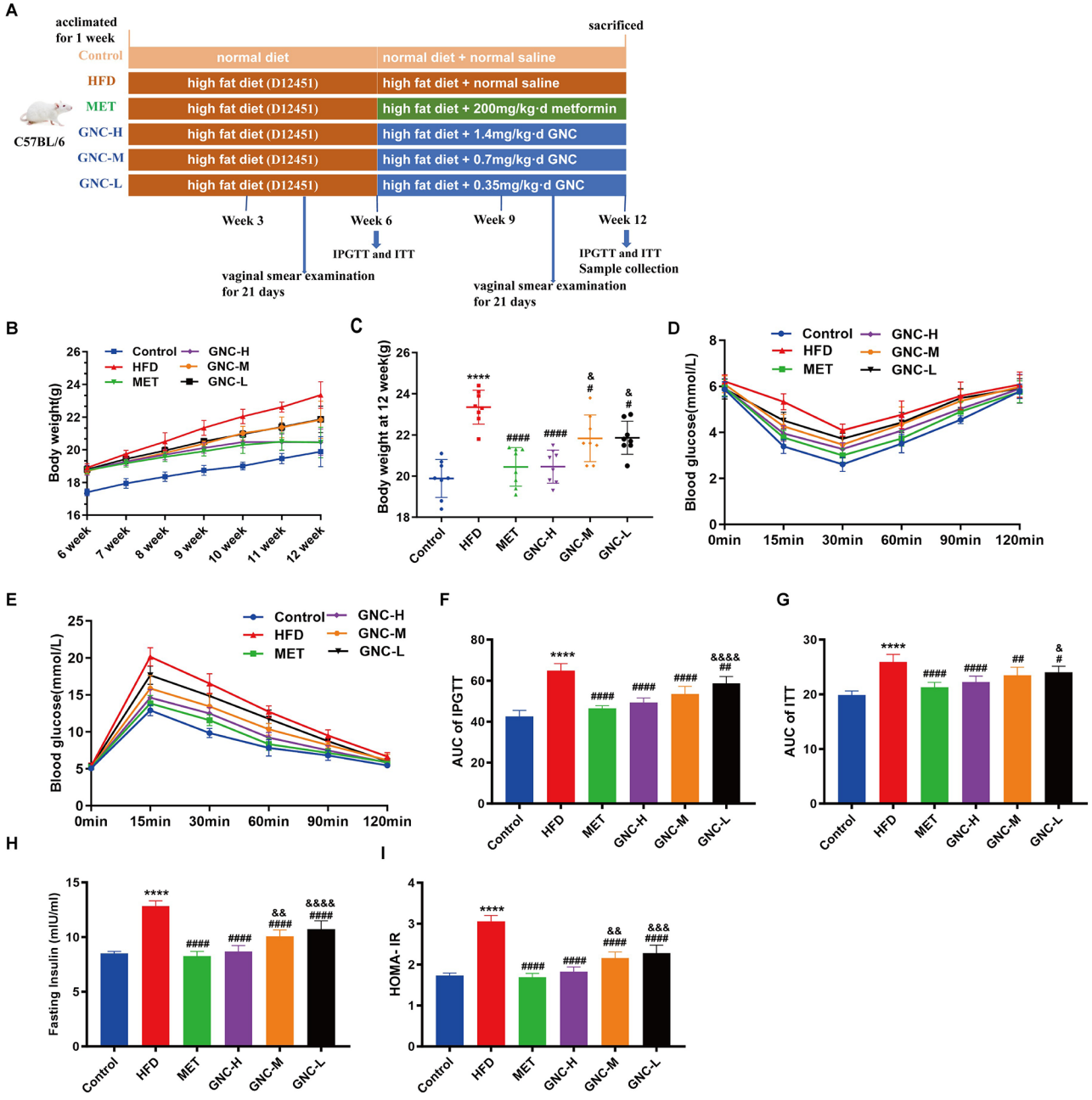

Fig. 5 GNC effectively alleviated insulin resistance in IR-induced DOR mice. (**A**) Experimental flow chart of therapeutic effect of GNC on IR-induced DOR. The IR-induced DOR model was established by 6-week HFD. The model was dministrated by gavage GNC at high, medium and low doses for 6 weeks, with metformin as a positive control group, while continuing the HFD. (**B**) Body weight changes of mice during the treatment for 6 weeks. (**C**) Final Body weight analysis of mice after GNC treatment. (**D-E**) IPGTT and ITT changes. (**F-G**) The AUC of IPGTT and ITT. (**H-I**) FINS and HOMA-IR. Data are shown as mean ± SD. $^{****}p < 0.001$ vs Control group; $^{\#}p < 0.05$, $^{\#\#}p < 0.01$, $^{\#\#\#\#}p < 0.0001$ vs. HFD group; $^{\&}p < 0.05$, $^{\&\&}p < 0.01$, $^{\&\&\&}p < 0.0001$, $^{\&\&\&\&}p < 0.0001$ vs GNC-H group

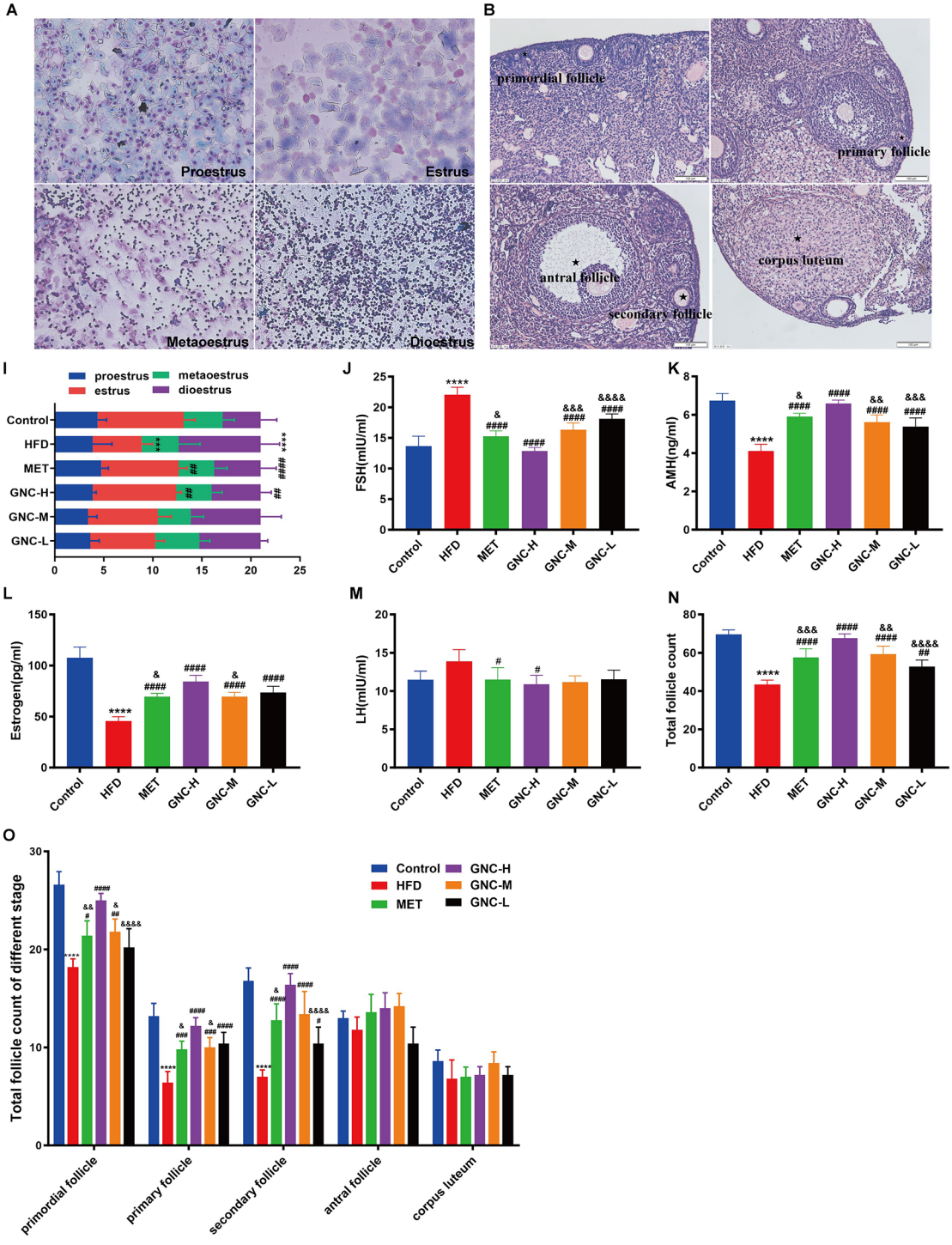

Fig. 6 GNC effectively improved the ovarian function in IR-induced DOR mice. (**A-D**) Vaginal smears of different estrous cycles. A: Proestrus, B:Estrus; C:Metaoestrus; D:Dioestrus. (**E-H**) Follicle morphology at different stages. E:★primordial follicle; F:★primary follicle; G★antral follicle, secondary follicle; H:★corpus luteum. (**I**) Estrus cycles; (J-M) Level FSH, LH, E_2, AMH.(**O**) Total Follicle count of different stage. $^{***}p<0.001$, $^{****}p<0.0001$vs Control group; $^{\#}p<0.05$, $^{\#\#}p<0.01$, $^{\#\#\#\#}p<0.0001$ vs. HFD group; $^{\&}p<0.05$, $^{\&\&\&\&}p<0.0001$ vs. GNC-H group

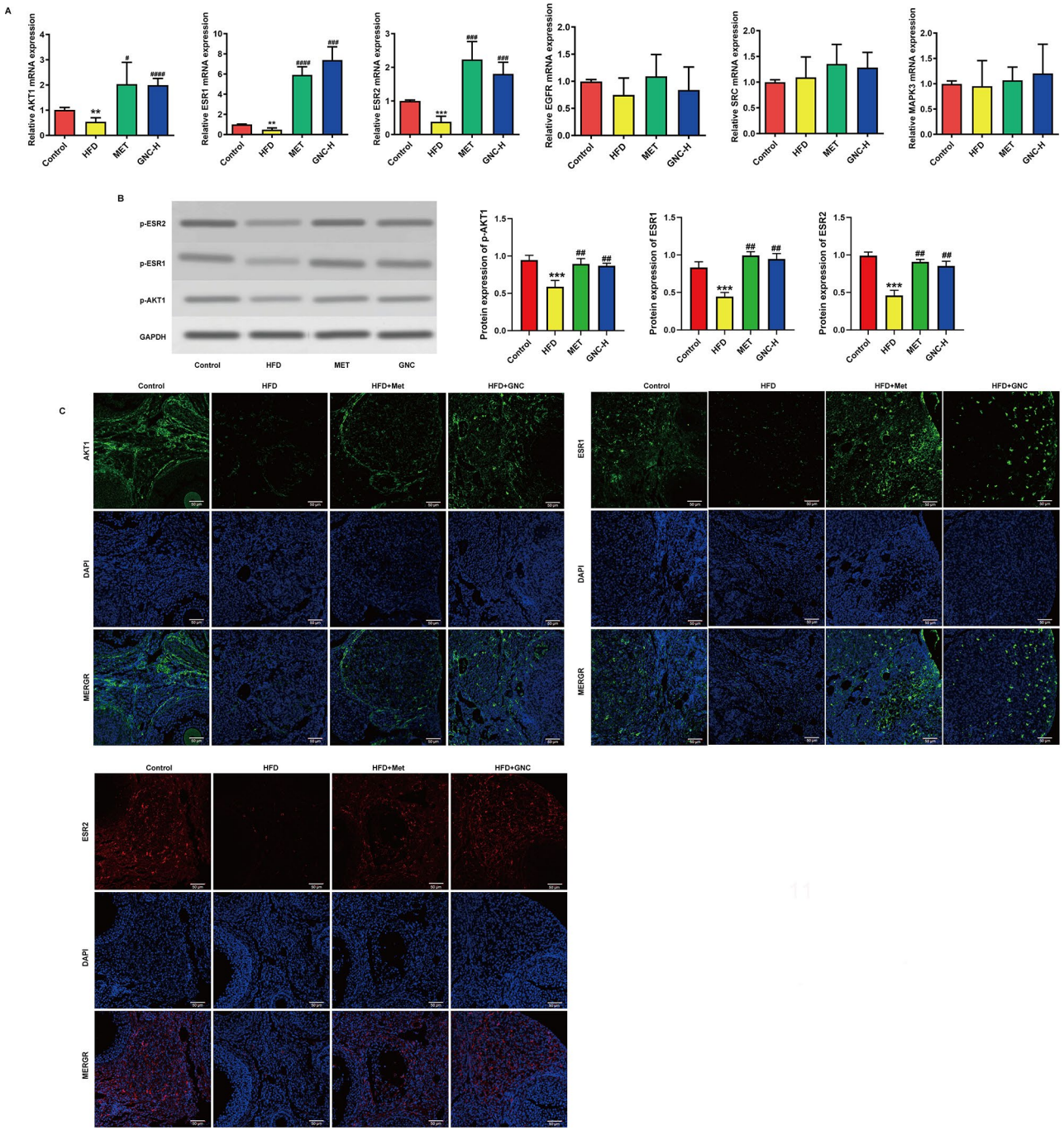

Fig. 7 GNC regulated the estrogen signaling pathway in IR-induced DOR mice. (**A**) mRNA expression of key genes involved in estrogen signaling: AKT1, ESR1, ESR2, EGFR, SRC, MAPK3, CTNNB1, ERBB2. (**B**) Western blot analysis of protein expression levels of p-AKT1, p-ESR1, and p-ESR2 in ovarian tissue. (**C**) Immunofluorescence staining showing enhanced expression of AKT1, ESR1, and ESR2 in GNC-treated ovarian tissues. Statistical significance: **$p < 0.01$, ***$p < 0.01$ vs Control group; #$p < 0.05$, ##$p < 0.01$, ###$p < 0.001$, ####$p < 0.0001$ vs HFD group

detected, with icariin from epimedium and berberine from Coptis standing out for their insulin-sensitizing and anti-inflammatory properties [24, 25]. In negative ion mode, peaks corresponding to organic oxygen compounds, including phenolic acids and lignans, were identified. Phenolic acids are well-known for their antioxidant and anti-inflammatory effects, while lignans contribute to metabolic regulation and hormonal balance [26]. These findings suggest that the bioactive compounds in GNC target multiple biological pathways, including insulin sensitivity, inflammation, and oxidative stress, all of which are crucial for improving insulin resistance and ovarian health. Furthermore, the UPLC-Q-TOF-MS/MS analysis of blood plasma after GNC administration confirmed the absorption of these active components into the bloodstream, validating their bioavailability and systemic effects. Among the key compounds identified, icariin, a flavonoid from Epimedium, plays a critical role in improving glucose metabolism by modulating key signaling pathways, such as AMPK and PI3K/Akt [27, 28]. Similarly, berberine, an alkaloid from Coptis, has been extensively studied for its ability to enhance insulin sensitivity, regulate glucose metabolism, and reduce inflammatory cytokines, contributing to the management of IR [29]. Additionally, paeoniflorin, a compound extracted from Paeonia lactiflora, has demonstrated the ability to reduce oxidative stress and promote granulosa cell proliferation, thus improving ovarian function and mitigating the detrimental effects of oxidative damage to the ovaries [30]. Together, these compounds contribute to GNC's holistic approach in managing insulin resistance and improving ovarian health, offering a multi-target strategy for treating IR-induced DOR.

The results from network pharmacology further elucidated the molecular mechanisms by which GNC improves IR and restores DOR. Using bioinformatics tools, we identified key molecular targets and signaling pathways likely involved in GNC's therapeutic effects. The GO and KEGG pathway enrichment analyses further highlighted the importance of estrogen signaling, supporting the hypothesis that GNC exerts its effects through modulation of ESR1 and ESR2. Previous experimental findings have confirmed that GNC can protect hippocampal neurons in rats by promoting ESR2 and influencing the PI3K/AKT signaling pathway [31]. To validate the findings from network pharmacology, we established a high-fat diet-induced IR and DOR mouse model. Metformin, a recognized insulin sensitizer, was used as a positive control. The experimental results showed that GNC effectively improved insulin sensitivity and restored ovarian function in IR-induced DOR mice. Notably, GNC demonstrated comparable or even superior efficacy to metformin, despite a significantly lower dosage. This can be attributed to the multi-target and multi-pathway nature of TCM. Unlike metformin, which mainly targets insulin resistance, GNC addresses multiple biological pathways, including insulin sensitivity, inflammation, oxidative stress, and estrogen signaling, contributing to a more comprehensive regulation of both metabolic and reproductive health. This broader action is particularly beneficial in treating IR-induced DOR, where insulin resistance and ovarian dysfunction are intertwined. The holistic and synergistic effects of GNC offer significant advantages over metformin, providing a more integrated therapeutic approach to improving insulin resistance and ovarian function, especially at a lower dosage. These findings support the potential of GNC as a promising alternative to conventional therapies for IR-induced DOR.

While this study provides valuable insights into the therapeutic potential of GNC, several limitations should be addressed in future research. First, the experimental validation of GNC's bioactive compounds was primarily carried out using animal models, which may not fully replicate the complexities of human physiology. Therefore, clinical trials involving human subjects are essential to confirm the efficacy and safety of GNC in treating IR and DOR. Second, although the UPLC-Q-TOF-MS/MS analysis provided valuable data on the bioactive compounds absorbed into the bloodstream, this study represents preliminary data. Further studies should focus on comparing these results with known standards to identify the drug metabolism processes of the active ingredients more comprehensively. Additionally, the current study primarily examined the metabolic components of GNC in the blood, while ovarian tissue analysis was not included. Future research should incorporate high-throughput detection of these bioactive components in ovarian tissue to provide a more thorough understanding of how GNC modulates ovarian reserve at the cellular and molecular levels.

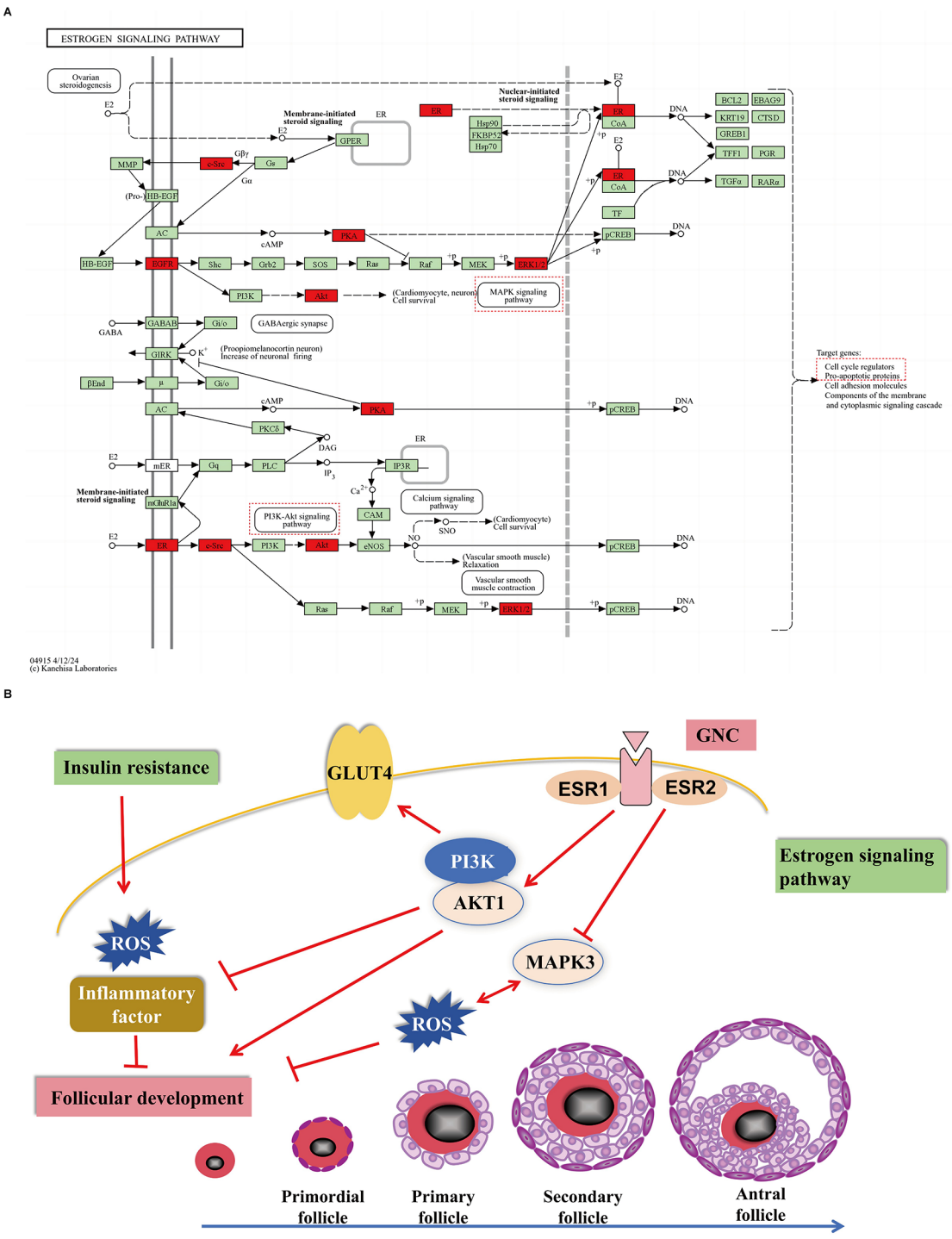

Fig. 8 Molecular mechanism of GNC against IR-induced DOR. (**A**) Key targets involved in the estrogen signaling pathway. (**B**) Schematic of the therapeutic effects of GNC in regulating insulin sensitivity and promoting ovarian function

Conclusion

In summary, this study elucidates the molecular mechanisms by which GNC enhances insulin sensitivity and mitigates IR-induced DOR. GNC activates estrogen signaling and the PI3K/AKT pathway, thereby enhancing insulin sensitivity, promoting follicular development, and restoring ovarian function (Fig. 8). These findings establish a solid foundation for subsequent clinical research and underscore the potential of GNC as an innovative therapeutic strategy for addressing IR-induced DOR.

Abbreviations

AKT	Serine-threonine kinase B
AMH	Anti-mullerian hormone
AMPK	Adenosine monophosphate-activated protein kinase
AUC	Area under the curve
BP	Biological processes
CC	Cellular components
DOR	Diminished ovarian reserve
E2	Estrogen
ESR	Estrogen receptor
FBG	Fasting blood glucose
FINS	Fasting insulin
FSH	Follicle-stimulating hormone
GNC	Gengnianchun
HFD	High fat diet
HOMA-IR	Homeostasis model assessment of insulin resistance
HPLC	High Performance Liquid Chromatography
IPGTT	Intraperitoneal glucose tolerance
IR	Insulin resistance
ITT	Insulin torlance test
LH	Luteinizing hormone
LC-MS	Liquid chromatograph mass spectrometer
MAPK	Mitogen-activated protein kinase
MF	Molecular functions
PI3K	Phosphatidylinositol 3-kinase
TCM	Traditional Chinese medicine
UPLC-Q-TOF-MS/MS	Ultra Performance Liquid Chromatography Quadrupole Time of flight Mass Spectrometry

Supplementary Information

The online version contains supplementary material available at https://doi.org/10.1186/s13048-025-01632-3.

Supplementary Material 1

Supplementary Material 2

Author contributions

Yanqiu Rao and Jun Li contributed equally to this work. Wenjun Wang: Experimental guidance and supervision. Yanqiu Rao and Jun Li: Experimental design, biological experiments, writing original draft. Yan Ding: Biological experiments, data analysis. Ting Xu: Date analysis. Lingyun Gao: performed phytochemical analysis. All authors reviewed the manuscript.

Funding

This work was supported by the National Natural Science Foundation of China (Grant number 8207140968) and the Science and Technology Innovation Plan Of Shanghai Science and Technology Commission (Grant number 23Y11920300).

Data availability

No datasets were generated or analysed during the current study.

Declarations

Competing interests

The authors declare no competing interests.

Author details

[1]Department of Integrated Traditional & Western Medicine, Obstetrics and Gynecology Hospital of Fudan University, Shanghai, China
[2]Department of Integrated Traditional & Western Medicine, Shanghai Key Laboratory of Female Reproductive Endocrine Related Diseases, Shanghai, China

Received: 5 January 2025 / Accepted: 19 February 2025
Published online: 11 March 2025

References

1. Kawamura K, Ishizuka B, Hsueh AJW. Drug-free in-vitro activation of follicles for infertility treatment in poor ovarian response patients with decreased ovarian reserve. Reprod Biomed Online. 2020;40(2):245–53.
2. Devine K, Mumford SL, Wu M, DeCherney AH, Hill MJ, Propst A. Diminished ovarian reserve in the united States assisted reproductive technology population: diagnostic trends among 181,536 cycles from the society for assisted reproductive technology clinic outcomes reporting system. Fertil Steril. 2015;104(3):612–e193.
3. Bunnewell SJ, Honess ER, Karia AM, Keay SD, Al Wattar BH, Quenby S. Diminished ovarian reserve in recurrent pregnancy loss: a systematic review and meta-analysis. Fertil Steril. 2020;113(4):818–e273.
4. Park SU, Walsh L, Berkowitz KM. Mechanisms of ovarian aging. Reprod (Cambridge England). 2021;162(2):R19–33.
5. Díaz-Hernández V, Montaño LM, Caldelas I, Marmolejo-Valencia A. A High-Fat and High-Carbohydrate diet promotes reminiscent hallmarks of an aging ovary in the rabbit model. Biomedicines. 2022;10(12).
6. Saltiel AR. Insulin signaling in health and disease. J Clin Invest. 2021;131(1).
7. Li L, Shi X, Shi Y, Wang Z. The signaling pathways involved in ovarian follicle development. Front Physiol. 2021;12:730196.
8. Paula VG, Sinzato YK, Gallego FQ, Cruz LL, Aquino AM, Scarano WR et al. Intergenerational hyperglycemia impairs mitochondrial function and follicular development and causes oxidative stress in rat ovaries independent of the consumption of a High-Fat diet. Nutrients. 2023;15(20).
9. Masenga SK, Kabwe LS, Chakulya M, Kirabo A. Mechanisms of oxidative stress in metabolic syndrome. Int J Mol Sci. 2023;24(9).
10. Huang Y, Cheng Y, Zhang M, Xia Y, Chen X, Xian Y, et al. Oxidative stress and inflammatory markers in ovarian follicular fluid of women with diminished ovarian reserve during in vitro fertilization. J Ovarian Res. 2023;16(1):206.
11. Dai F, Liu H, He J, Wu J, Yuan C, Wang R, et al. Model construction and drug therapy of primary ovarian insufficiency by ultrasound-guided injection. Stem Cell Res Ther. 2024;15(1):49.
12. Liu J, Wei B, Ma Q, Shi D, Pan X, Liu Z, et al. Network Pharmacology and experimental validation on Yangjing Zhongyu Decoction against diminished ovarian reserve. J Ethnopharmacol. 2024;318(Pt B):117023.
13. Zhang QL, Lei YL, Deng Y, Ma RL, Ding XS, Xue W, et al. Treatment progress in diminished ovarian reserve: Western and Chinese medicine. Chin J Integr Med. 2023;29(4):361–7.
14. Zhang X, Zhang L, Xiong L, Liu X, Zhang J, Yu F, et al. Kuntai capsule for the treatment of diminished ovarian reserve: A systematic review and meta-analysis of randomized controlled trials. J Ethnopharmacol. 2024;329:118167.
15. Rao Y, Wang Y, Li J, Wang W. In: Rao Y, Wang Y, Li J, Wang W, editors. Clinical research on the effect of integrated traditional Chinese and Western medicine in treatment of infertile patients with diminished ovarian reserve function. Fudan University Journal Medical science.; 2019. pp. 750–4.
16. Gao H, Gao L, Rao Y, Qian L, Li M, Wang W. The Gengnianchun recipe attenuates insulin resistance-induced diminished ovarian reserve through inhibiting the senescence of granulosa cells. Front Endocrinol. 2023;14:1133280.
17. Stoner CL, Gifford E, Stankovic C, Lepsy CS, Brodfuehrer J, Prasad JV, et al. Implementation of an ADME enabling selection and visualization tool for drug discovery. J Pharm Sci. 2004;93(5):1131–41.
18. Lipinski CA, Lombardo F, Dominy BW, Feeney PJ. Experimental and computational approaches to estimate solubility and permeability in drug discovery and development settings. Adv Drug Deliv Rev. 2001;46(1–3):3–26.
19. Bardou P, Mariette J, Escudié F, Djemiel C, Klopp C. Jvenn: an interactive Venn diagram viewer. BMC Bioinformatics. 2014;15(1):293.
20. Oktay K, Schenken RS, Nelson JF. Proliferating cell nuclear antigen marks the initiation of follicular growth in the rat. Biol Reprod. 1995;53(2):295–301.
21. Han Y, Wu H, Sun S, Zhao R, Deng Y, Zeng S et al. Effect of high fat diet on disease development of polycystic ovary syndrome and lifestyle intervention strategies. Nutrients. 2023;15(9).
22. Lotti F, Marchiani S, Corona G, Maggi M. Metabolic syndrome and reproduction. Int J Mol Sci. 2021;22(4).
23. Jinno M, Nagai R, Takeuchi M, Watanabe A, Teruya K, Sugawa H, et al. Trapa bispinosa Roxb. Extract lowers advanced glycation end-products and increases live births in older patients with assisted reproductive technology: a randomized controlled trial. Volume 19. Reproductive biology and endocrinology: RB&E; 2021. p. 149. 1.
24. Nie X, Sheng W, Hou D, Liu Q, Wang R, Tan Y. Effect of Hyperin and Icariin on steroid hormone secretion in rat ovarian granulosa cells. Clin Chim Acta. 2019;495:646–51.

25. Peng Y, Sun L, Guo W, Liu Z, Wang T, Zou T, et al. Berberine protects cyclophosphamide and busulfan-induced premature ovarian insufficiency in mouse model. J Pharmacol Sci. 2023;153(1):46–54.
26. Yahfoufi N, Alsadi N, Jambi M, Matar C. The Immunomodulatory and Anti-Inflammatory role of polyphenols. Nutrients. 2018;10(11).
27. Chen SQ, Ding LN, Zeng NX, Liu HM, Zheng SH, Xu JW, et al. Icariin induces irisin/FNDC5 expression in C2C12 cells via the AMPK pathway. Volume 115. Biomedicine & pharmacotherapy = Biomedecine & pharmacotherapie.; 2019. p. 108930.
28. Li X, Wang YX, Shi P, Liu YP, Li T, Liu SQ, et al. Icariin treatment reduces blood glucose levels in type 2 diabetic rats and protects pancreatic function. Experimental Therapeutic Med. 2020;19(4):2690–6.
29. Zhang N, Liu X, Zhuang L, Liu X, Zhao H, Shan Y, et al. Berberine decreases insulin resistance in a PCOS rats by improving GLUT4: dual regulation of the PI3K/AKT and MAPK pathways. Regul Toxicol Pharmacology: RTP. 2020;110:104544.
30. Ren S, Wang Y, Zhang Y, Yan P, Xiao D, Zhao Y, et al. Paeoniflorin alleviates AngII-induced cardiac hypertrophy in H9c2 cells by regulating oxidative stress and Nrf2 signaling pathway. Volume 165. Biomedicine & pharmacotherapy = Biomedecine & pharmacotherapie.; 2023. p. 115253.
31. Zhang Y, Gao L, Wang W. Neuroprotective effect of herbal medicine Gengnianchun formula on primary cultured rat fetal hippocampal neurons injury induced by Aβ25–35 through ERβ and PI3K/Akt signalingpathway. Fudan Univ J Med Sci. 2020;47(01):66–75.

Publisher's note